

# PKM $\zeta$ traces hippocampal LTP maintenance and spatial long-term memory

## Authors:

Changchi Hsieh,<sup>1,\*</sup> Panayiotis Tsokas,<sup>1,2,\*</sup> Ain Chung,<sup>3,#</sup> Claudia Garcia-Jou,<sup>4</sup> Edith Lesburguères,<sup>3,§</sup> Nesha S. Burghardt,<sup>4</sup> Christine A. Denny,<sup>5</sup> Rafael E. Flores-Obando,<sup>1</sup> Laura Melissa Rodríguez Valencia,<sup>2</sup> Peter Bergold,<sup>1,6</sup> James E. Cottrell,<sup>2</sup> André Antonio Fenton,<sup>1,3</sup> Todd Charlton Sacktor<sup>1,2,6</sup>

## Affiliations:

<sup>1</sup>Department of Physiology and Pharmacology, The Robert F. Furchtgott Center for Neural and Behavioral Science, State University of New York Downstate Health Sciences University, Brooklyn, New York 11203, USA.

<sup>2</sup>Department of Anesthesiology, State University of New York Downstate Health Sciences University, Brooklyn, New York 11203, USA.

<sup>3</sup>Center for Neural Science, New York University, New York, New York 10003, USA.

<sup>4</sup>Department of Psychology, Hunter College, The City University of New York, New York and Department of Psychology, The Graduate Center, The City University of New York, New York 10065, USA

<sup>5</sup>Department of Psychiatry, Columbia University Irving Medical Center, Division of Systems Neuroscience, Research Foundation for Mental Hygiene, Inc., New York State Psychiatric Institute Kolb Research Annex, New York, New York 10032, USA

<sup>6</sup>Department of Neurology, State University of New York Downstate Health Sciences University, Brooklyn, New York 11203, USA.

**Keywords:** PKMzeta, PKM-zeta, ArcCreER<sup>T2</sup> x eYFP mice, memory storage

**Correspondence:** Todd Charlton Sacktor, as above.

E-mail: [tsacktor@downstate.edu](mailto:tsacktor@downstate.edu)

André Antonio Fenton, as above.

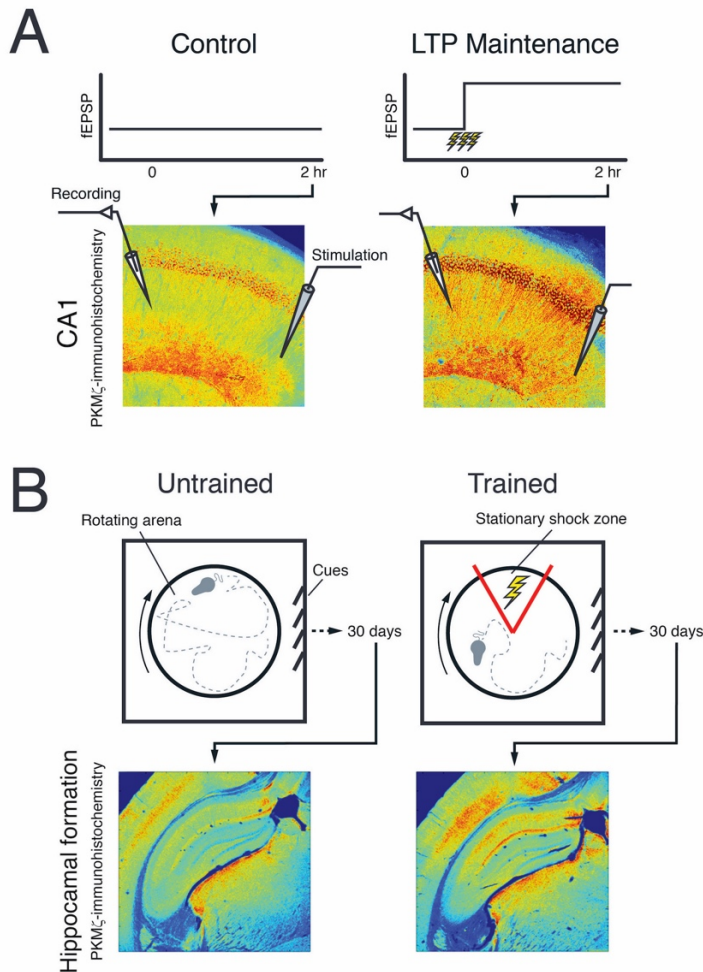
E-mail: [afenton@nyu.edu](mailto:afenton@nyu.edu)

\*These authors contributed equally.

#Present address: Center for Regenerative Medicine, Massachusetts General Hospital, Harvard Medical School, 185 Cambridge Street, MCPZN 4000, Boston, United States

§Present address: Centre National de La Recherche Scientifique, University of Bordeaux, Interdisciplinary Institute for Neuroscience, UMR 5297, 33000, Bordeaux, France

## Graphical Abstract



PKM $\zeta$ -immunohistochemistry reveals persistent increased PKM $\zeta$  in the hippocampus during (A) LTP maintenance, and (B) spatial long-term memory storage.

PKM $\zeta$  is an autonomously active, atypical PKC isoform crucial for maintaining synaptic long-term potentiation (LTP) and long-term memory. Unlike other PKCs that are transiently activated by short-lived second messengers, PKM $\zeta$  is persistently activated by long-lasting increases in the amount of the autonomously active kinase during LTP and long-term memory maintenance. Thus, localizing persistent increases in PKM $\zeta$  might reveal traces of physiological LTP maintenance in the circuitry of the brain during long-term memory storage. Using quantitative immunohistochemistry validated by the lack of staining in PKM $\zeta$ -null mice, we visualized the amount and distribution of PKM $\zeta$  during LTP maintenance and spatial long-term memory storage in the hippocampal formation of wild-type mice. Strong afferent stimulation of Schaffer collateral/commissural fibers inducing LTP maintenance increases PKM $\zeta$  in CA1 pyramidal cells for 2 hours in hippocampal slices. Active place avoidance spatial conditioning increases PKM $\zeta$  in CA1 pyramidal cells of the hippocampal formation from 1 day to at least 1 month. The increases in PKM $\zeta$  coincide with the location of cells marked during long-term memory training by Arc promoter-mediated expression of a fluorescent protein, including at dendritic spines. We conclude that increased PKM $\zeta$  forms persistent traces in CA1 pyramidal cells that are sites of molecular information storage during LTP maintenance and spatial long-term memory.

## Introduction

The persistent action of  $\text{PKM}\zeta$  is a leading candidate for a molecular mechanism of long-term memory storage (Sacktor & Fenton, 2018).  $\text{PKM}\zeta$  is a nervous system-specific, atypical PKC isoform with autonomous enzymatic activity (Sacktor *et al.*, 1993). The autonomous activity of  $\text{PKM}\zeta$  is due to its structure that differs from other PKC isoforms. Most PKCs consist of an autoinhibitory regulatory domain that suppresses the action of a catalytic domain. Therefore, these full-length isoforms are inactive unless second messengers bind to the regulatory domain and induce a conformational change that releases the autoinhibition. Because the increases in PKC second messengers, such as  $\text{Ca}^{2+}$  or diacylglycerol, typically last only seconds during signal transduction, most PKC isoforms are only transiently active.

$\text{PKM}\zeta$ , in contrast, consists of an independent  $\text{PKC}\zeta$  catalytic domain, which, lacking the autoinhibition of a regulatory domain, is autonomously and therefore persistently active.  $\text{PKM}\zeta$  is translated from a  $\text{PKM}\zeta$  mRNA, which is transcribed by an internal promoter within the  $\text{PKC}\zeta/\text{PKM}\zeta$  gene (*PRCKZ*) that is active only in neural tissue (Hernandez *et al.*, 2003).  $\text{PKM}\zeta$  mRNA is continually transported to the dendrites of neurons (Muslimov *et al.*, 2004), but under basal conditions is translationally repressed (Hernandez *et al.*, 2003). High-frequency afferent synaptic activity, such as during LTP induction or learning, derepresses the  $\text{PKM}\zeta$  mRNA, triggering new synthesis of  $\text{PKM}\zeta$  protein (Osten *et al.*, 1996; Hsieh *et al.*, 2017). The newly synthesized  $\text{PKM}\zeta$  then translocates to postsynaptic sites, where the kinase's autonomous activity potentiates transmission of synaptic pathways that had been previously activated, but not synaptic pathways that had been inactive, in a process known as “synaptic tagging and capture” (Sajikumar *et al.*, 2005; Palida *et al.*, 2015).

Once increased, the steady-state amount of  $\text{PKM}\zeta$  can remain elevated, and because increased amounts of the autonomous kinase are sufficient to maintain LTP, the persistent increase of  $\text{PKM}\zeta$  is thought to maintain LTP and long-term memory (Ling *et al.*, 2002; Pastalkova *et al.*, 2006; Tsokas *et al.*, 2016). In hippocampal slices, the increase of  $\text{PKM}\zeta$  in LTP maintenance measured by quantitative immunoblotting of microdissected CA1 regions persists for several hours, correlating with the degree of synaptic potentiation (Osten *et al.*, 1996; Tsokas *et al.*, 2016). *In vivo*, the increase in  $\text{PKM}\zeta$  during spatial long-term storage as measured by immunoblots of dorsal hippocampus persists from days to weeks, correlating with the degree and duration of memory retention (Hsieh *et al.*, 2017).

These findings suggest that visualizing the amount and distribution of  $\text{PKM}\zeta$  might reveal the location of the physiological maintenance mechanism of LTP within the dorsal hippocampus. Here we test this notion using quantitative immunohistochemistry to determine the sites of increased  $\text{PKM}\zeta$  during LTP maintenance and the storage of active place avoidance, a spatial memory that requires increases in  $\text{PKM}\zeta$  activity in the hippocampus and depends upon the hippocampus from 1 day to 1 month (Pastalkova *et al.*, 2006; Tsokas *et al.*, 2016; Hsieh *et al.*, 2017).

## Materials and Methods

**Reagents.** The  $\zeta$ -specific rabbit anti- $\text{PKM}\zeta$  C-2 polyclonal antiserum (1:10,000 for immunohistochemistry; 1:20,000 for immunoblots) was generated as previously described

(Hernandez *et al.*, 2003). Actin (1:5000) mouse monoclonal Ab and other reagents unless specified were from Sigma. Protein concentrations were determined using the Bio-Rad RC-DC Protein Assay kit (Bio-Rad), with bovine serum albumin as standard.

#### *Hippocampal slice preparation and recording*

Acute mouse hippocampal slices (450  $\mu$ m) were prepared with a McIlwain tissue slicer as described previously (Tsokas *et al.*, 2005; Tsokas *et al.*, 2019), and maintained in an Oslo-type interface recording chamber at 31.5 °C for at least 2 h before recording. Field excitatory postsynaptic potentials (fEPSPs) were recorded with a glass extracellular recording electrode (2–5 M $\Omega$ ) placed in the CA1 stratum radiatum, and concentric bipolar stimulating electrodes were placed within CA3. Synaptic efficiency was measured as the maximum slope of the fEPSP. The high-frequency stimulation consisted of standard two 100 Hz-1sec tetanic trains, at 25% of spike threshold, spaced 20 sec apart, which is optimized to produce a relatively rapid onset synthesis of PKM $\zeta$  and protein synthesis-dependent late-phase LTP (Osten *et al.*, 1996; Tsokas *et al.*, 2005). The slope from 10-90% of the rise of the fEPSP is analyzed on an IBM computer using the WinLTP data acquisition program (Anderson & Collingridge, 2007).

#### *Active place avoidance*

The place avoidance procedures have been described previously (Tsokas *et al.*, 2016). Briefly, the mouse is placed on a 40 cm diameter circular arena rotating at 1 rpm within a room, and the mouse position is determined 30 times per second by video tracking from an overhead camera with a PC (Tracker, Bio-Signal Group). A clear wall made from Polyethylene Terephthalate Glycol-modified (PET-G) prevented the animal from jumping off the elevated arena surface. This task challenges the animal on the rotating arena to avoid an unmarked 60° sector shock zone that is defined by distal visual landmarks in the room. When the system detects the mouse in the shock zone for 500 ms, a mild constant current foot-shock (60 Hz, 500 ms, 0.2 mA), minimally sufficient to make the animal move, is delivered and repeated each 1500 ms until the mouse leaves the shock zone. During a training trial, the arena rotation periodically transports the animal into the shock zone, and the mouse is forced to actively avoid it. In addition, a pretraining habituation trial and a posttraining memory retention test are conducted for the equivalent time to a training session, but without shock. The time to first enter the shock zone in each trial is recorded as an index of between-session memory.

In the 1-day memory retention task (Fig. 2), the mouse first receives a 30 min habituation trial without shocks, followed by three 30 min training trials with a 2 h inter-trial interval (ITI). The memory is tested 24 h later. In the 1-week memory retention task (Supplementary Fig. 1), the mouse first receives a 30 min habituation trial without shocks on Day 1, followed by three daily 30 min training trials. The memory is tested 7 days after the last training trial. In the 1-month memory retention task (Fig. 4), the mouse first receives a 30 min habituation trial without shocks, followed by three 30 min training trials with 2 h ITI. Another three training trials are conducted 10 days later, and the memory is tested 30 days after the last training trial.

#### *Preparation of hippocampal extracts*

Immediately after training, dorsal hippocampal extracts were prepared for immunoblots. The hippocampi of 2–3 month-old, male C57BL/6J mice were removed after decapitation under deep isofluorane-induced anesthesia into ice-cold artificial cerebrospinal fluid with high Mg<sup>2+</sup>

(10 mM) and low Ca<sup>2+</sup> (0.5 mM) (Sacktor *et al.*, 1993), according to State University of New York Downstate Health Sciences University Animal Use and Care Committee standards. All efforts were made to minimize animal suffering and to reduce the number of animals used. The dorsal hippocampus consisting of 50% of the hippocampus from the septal end was dissected out, snap-frozen and stored in a microcentrifuge tube at -80°C until lysis. Dorsal hippocampi were lysed directly in the microcentrifuge tube using a motorized homogenizer, as previously described (Tsokas *et al.*, 2005; Tsokas *et al.*, 2016). Each dorsal hippocampus was homogenized in 100  $\mu$ L of ice-cold modified ice-cold RIPA buffer consisting of the following (in mM, unless indicated otherwise): 25 Tris-HCl (pH 7.4), 150 NaCl, 6 MgCl<sub>2</sub>, 2 EDTA, 1.25% NP-40, 0.125% SDS, 0.625% Na deoxycholate, 4 *p*-nitrophenyl phosphate, 25 Na fluoride, 2 Na pyrophosphate, 20 dithiothreitol (DTT), 10  $\beta$ -glycerophosphate, 1  $\mu$ M okadaic acid, phosphatase inhibitor cocktail I & II (2% and 1%, respectively, Calbiochem), 1 phenylmethylsulfonyl fluoride (PMSF), 20  $\mu$ g/ml leupeptin, and 4  $\mu$ g/ml aprotinin.

#### *Immunoblotting*

Methods used were described previously (Tsokas *et al.*, 2005; Tsokas *et al.*, 2016). Appropriate volumes of 4X NuPage LDS Sample Buffer (Invitrogen, Carlsbad, CA) and  $\beta$ -mercaptoethanol were added to the homogenates, and the samples were boiled for 5 min. Samples were loaded (15-20  $\mu$ g of protein per well) in a 4–20% Precast Protein Gel, (Biorad) and resolved by SDS-PAGE. Following transfer at 4°C, nitrocellulose membranes (pore size, 0.2  $\mu$ m; Invitrogen) were blocked for at least 30 min at room temperature with blocking buffer (BB: 5% non-fat dry milk in TBS containing 0.1% Tween 20 [TBS-T]; or Licor Odyssey Blocking Buffer), then probed overnight at 4°C using primary antibodies dissolved in BB or Licor Odyssey Blocking Buffer with 0.1% Tween 20 and 0.01 % SDS. After washing in TBS-T (or PBS + 0.1% Tween 20 [PBS-T]; 3 washes, 5 min each), the membranes were incubated with IRDye (Licor) secondary antibodies. Proteins were visualized by the Licor Odyssey System. Densitometric analysis of the bands was performed using NIH ImageJ, and values were normalized to actin.

#### *Immunohistochemistry and confocal microscopy*

Brains were fixed by cardiac perfusion and hippocampal slices were placed in ice-cold 4% paraformaldehyde in 0.1 M phosphate buffer (PB, pH 7.4) immediately after behavioral testing or recording, and post-fixed for 48 hr. Slices were then washed with PBS (pH 7.4) and cut into 40  $\mu$ M sections using a Leica VT 1200S vibratome. As previously described (Tsokas *et al.*, 2005; Tsokas *et al.*, 2007), free-floating sections were permeabilized with PBS-T for 1 h at room temperature and blocked with 10% normal donkey serum in PBS-T for 2.5 h at room temperature. The sections were then incubated overnight at 4°C with primary antibody rabbit anti-PKM $\zeta$  C-2 antisera (1:10,000) in 5% normal goat serum in PBS-T. After washing 6 times for 10 mins each in PBS-T, the sections were then incubated in 5% normal goat serum in PBST with secondary antibody biotinylated donkey anti-rabbit (1:250) (Jackson ImmunoResearch) for 2 h at room temperature. Following washing 6 times for 10 mins each in PBS-T, the sections were then incubated in 5% normal goat serum in PBS-T with streptavidin conjugated-Alexa 647 (1:250) (Jackson ImmunoResearch) for 2 h at room temperature. After extensive washing with PBS-T, the sections were mounted with DAPI Fluoromount-G (Southern Biotech) and imaged using an Olympus Fluoview FV1000 and Zeiss LSM 800 confocal microscopes at 4X, 10X, or 60X magnification. All parameters (pinhole, contrast and brightness) were held constant for all sections from the same experiment. To compare the intensity profile of PKM $\zeta$ -immunostaining

between images, we converted the images into grayscale and used the MATLAB functions '*imread*' and '*imagesc*' to scale the intensity distribution into the full range of a colormap. The same colormaps were used when comparing pairs of images, and representative colormaps are provided in the figures.

#### *Genetic tagging of memory-activated cells*

##### *ArcCreER<sup>T2</sup> x eYFP mice and ArcCreER<sup>T2</sup> x ChR2-eYFP mice*

ArcCreER<sup>T2</sup>(+) (Denny *et al.*, 2014) x R26R-STOP-floxed-eYFP (enhanced yellow fluorescent protein) (Srinivas *et al.*, 2001) and ArcCreER<sup>T2</sup>(+) x R26R-STOP-floxed-ChR2-eYFP (homozygous female mice) were bred with R26R-STOP-floxed-eYFP and R26R-STOP-floxed-ChR2-eYFP (Perusini *et al.*, 2017; Lacagnina *et al.*, 2019) homozygous male mice, respectively (Srinivas *et al.*, 2001). All experimental mice were ArcCreER<sup>T2</sup>(+) and homozygous for the eYFP or Chr2-eYFP reporter.

#### *Genotyping*

Genotyping was performed as previously described (Denny *et al.*, 2014).

#### *Memory Trace Tagging*

For memory trace tagging experiments, mice were housed in a separate isolation room in a fresh cage (2 mice/cage) in continuous darkness, 1-2 days before the pretraining trial to prevent unnecessary disturbances and reduce off-target labeling. One day after the pretraining trial, three 30-min training trials with 2.5 hr ITI were conducted. The next day, mice were injected with tamoxifen (TAM; 2 mg in 200  $\mu$ l i.p., Sigma, St. Louis, MO, H7904), which is required for Cre recombinase activation (Denny *et al.*, 2014), and administered a fourth 30 min place avoidance training 5 h later (Fig. 3A) or 4OH-TAM and trained 45 min later (Fig. 3B). Following the behavioral task, mice were housed in the isolation room for the next 3 days. The mice were then taken out of the isolation, their cages changed, and they were returned to the normal colony room. After 2 days in the colony room, memory retention was tested. All precautions to prevent disturbances to the mice during isolation housing were taken in order to reduce off-target labeling.

#### *Expansion microscopy*

The density of ChR2-eYFP expression in the neuropil is excessive, making it difficult to evaluate the organization of immunohistochemically-identified PKM $\zeta$  puncta at spines from single neurons (labeling with eYFP alone tags neurons but not the entirety of their processes). We therefore used expansion microscopy according to the published procedure (Chen *et al.*, 2015) to isometrically enlarge the tissue sample 4.5 times. This optimizes the ChR2-eYFP optical density for confocal microscopic analysis of PKM $\zeta$ , which at this high resolution appears as puncta in dendrites and spines.

#### *Statistics*

All statistical analyses are performed by Statistica software (StatSoft, OK). For LTP experiments, paired Student's *t* tests are performed to compare the average of 5 min responses at the time points before and 120 min after the tetanization. Multi-level comparisons are performed by one-way ANOVA, and multi-factor comparisons are performed by ANOVA with

repeated measures, as appropriate. The degrees of freedom for the critical  $t$  values of the  $t$  tests and the  $F$  values of the ANOVAs are reported as subscripts. Post-hoc multiple comparisons are performed by Fisher's least significant difference (LSD) tests as appropriate. Statistical significance is accepted at  $P < 0.05$ .

## Results

### *Persistent increased PKM $\zeta$ in LTP maintenance*

We first examined the amount and distribution of PKM $\zeta$  after strong afferent stimulation that induces late-LTP in hippocampal slices of wild-type mice. We tetanized Schaffer collateral/commissural fibers and recorded enhanced fEPSPs in CA1 radiatum for 2 h (Fig. 1A). Comparing the average responses of the 5 min before tetanization, LTP maintenance persists for 2 h post-tetanization ( $n = 4$ ,  $t_3 = 8.70$ ,  $P = 0.003$ ). For quantitation of immunohistochemistry, we determined the extent that non-PKM $\zeta$  background staining contributes to immunostaining with PKM $\zeta$ -antiserum by comparing immunostaining of hippocampi from the wild-type mice to *Prkcz*-null mice that lack PKM $\zeta$  (PKM $\zeta$ -null mice) (Tsokas *et al.*, 2016). PKM $\zeta$ -null mice show minimal background immunostaining (Fig. 1B, left), equivalent to the low level of staining in alveus of wild-type mice (Hernandez *et al.*, 2014) (Fig. 1B, middle), which was set as the level of background. Immunostaining for PKM $\zeta$  in the tetanized slices was then compared to control slices from the same hippocampus that received test stimulation for equivalent periods of time. The results reveal increased PKM $\zeta$  in CA1 pyramidal cells during LTP maintenance (Fig. 1B, right, C). Comparing the PKM $\zeta$ -immunostaining intensity profiles in CA1 regions of untetanized controls to those with LTP maintenance (Fig. 1C), the area under the LTP profile is significantly larger ( $n$ 's = 4,  $t_6 = 3.31$ ,  $P = 0.016$ ). By inspection, the increase extends from adjacent to the stimulating electrode in the CA3/CA1 border to the subiculum.

### *Persistent increased PKM $\zeta$ in spatial long-term memory storage*

We next examined the amount and distribution of PKM $\zeta$  in the hippocampal formation during spatial long-term memory storage. Untrained animals were placed in the apparatus for equivalent periods of time as trained animals, but received no shock (Fig. 2A). Because the only physical difference in the environment for trained and untrained mice is the 500-ms during a shock (< 1% of the total training experience), because the trained mice express the conditioned response and the untrained mice do not (Fig. 2A), and because corticosterone levels do not differ between trained and untrained mice, the untrained mice serve as a control (Lesburgueres *et al.*, 2016). Wild-type mice were trained by a 30-min habituation trial, followed by three 30-min training trials with 2 h intertrial intervals. Memory was tested one day later. Significant effects are of training phase ( $F_{2,28} = 12.62$ ,  $P = 0.00012$ ), treatment (control and trained) ( $F_{1,14} = 48.99$ ,  $P < 0.0001$ ), as well as their interaction ( $F_{2,28} = 13.46$ ,  $P < 0.0001$ ). The retention performance is significantly different by post-hoc test,  $P < 0.0001$ ; control,  $n = 10$ , trained,  $n = 6$ ).

One day after mice were conditioned to form an active place avoidance memory, PKM $\zeta$  was examined by quantitative immunoblot or immunohistochemistry. In line with previous work using quantitative immunoblots of rat hippocampus 1 day after spatial training (Hsieh *et al.*, 2017), immunoblots of mouse hippocampus 1 day after spatial training show persistent increases in PKM $\zeta$  compared to untrained control mice (Fig. 2B;  $t_{14} = 2.47$ ,  $P = 0.027$ ; control,  $n = 10$ , trained,  $n = 6$ ).

We then examined trained and untrained mice by immunohistochemistry (Fig. 2C). Compared to untrained control mice that experienced the same environment as the trained mice but were not shocked, by inspection we observe prominent increases in PKM $\zeta$  in hippocampus subfield CA1, in particular in *strata pyramidale*, *radiatum*, and *lacunosum-moleculare*. In contrast, increases in PKM $\zeta$  are less obvious in dentate gyrus (DG) and are not detectable in subfield CA3. Outside the hippocampal formation, increased PKM $\zeta$  is observed in overlying somatosensory and parietal association neocortex, at the superficial as well as the deep layers, but not retrosplenial cortex, nor in thalamus.

Quantitation of PKM $\zeta$ -immunostaining along profiles extending across CA1, CA3, and DG subfields reveals training is associated with increased PKM $\zeta$  across the entire profile of CA1, as compared to CA3 or DG (Fig. 2D). ANOVA reveals the main effects of treatment (control and trained,  $F_{1,10} = 8.89, P = 0.014$ ), region (CA1, DG, and CA3,  $F_{2,20} = 167.77, P < 0.0001$ ), and interaction between treatment and region ( $F_{2,20} = 10.32, P = 0.0008$ ). Post-hoc tests show that PKM $\zeta$  of the trained group is increased in CA1, but not DG or CA3, compared to untrained control group ( $n$ 's = 6,  $P < 0.0001, P = 0.34, P = 0.74$ , respectively). We therefore subsequently focused on characterizing the changes of PKM $\zeta$  in CA1 in spatial memory.

To determine whether experience in the place avoidance apparatus without training contributes to the increase in PKM $\zeta$  in CA1, we examined 3 groups: homecage control mice, untrained control mice placed in the apparatus without shock, and trained mice. To examine a more persistent spatial memory, we spaced the 3 training trials over 3 days, and then quantitated PKM $\zeta$  immunohistochemistry 1 week later (Supplementary Fig. 1) (Chung *et al.*, 2019). ANOVA for the untrained and trained groups reveals significant effects of training phase (pretraining, the end of training, and retention,  $F_{2,22} = 19.69, P < 0.0001$ ), treatment (untrained and trained,  $F_{1,11} = 29.49, P = 0.0002$ ), and their interaction ( $F_{2,22} = 17.42, P < 0.0001$ ). The 1-week retention performance is significantly different (post-hoc test,  $P < 0.0001$ ; untrained,  $n = 6$ , trained,  $n = 7$ ).

The CA1 PKM $\zeta$  intensities from different treatments (homecage control, untrained control, and trained) were then analyzed by ANOVA, which shows a treatment main effect ( $F_{2,17} = 5.16, P = 0.018$ ; home cage,  $n = 7$ , untrained,  $n = 6$ , trained,  $n = 7$ ). Post-hoc tests reveal that the trained group has higher CA1 PKM $\zeta$  intensity than the untrained and homecage groups ( $P = 0.033, P = 0.007$ , respectively), and there is no statistical difference between homecage and untrained ( $P = 0.54$ ).

### *PKM $\zeta$ in memory-tagged cells in CA1*

To examine the subcellular location of PKM $\zeta$  traces within CA1 pyramidal cells we took advantage of mice in which fluorescent proteins permanently tags cells, if the cells were active during the formation of a memory. We first used the ArcCreER<sup>T2</sup> x eYFP mice, the result of a cross between an ArcCreER<sup>T2</sup> mouse that will generate Cre-recombinase under control of the immediate early gene Arc promoter, but only in the presence of tamoxifen, and a R26R-STOP-floxed-eYFP mouse that will transcribe eYFP at the Rosa26 locus. In these mice, Cre recombination occurs only in cells with activated Arc transcription, as during training, and after administration of tamoxifen (2 mg in 200  $\mu$ l i.p.). The Cre recombinase then removes a floxed STOP codon, permitting the cells to permanently synthesize the reporter protein (Srinivas *et al.*, 2001; Denny *et al.*, 2014).

Tamoxifen injections during training causes memory-associated tagging of a minority of hippocampal neurons (Fig. 3A), as expected from prior work (Guzowski *et al.*, 1999; Guzowski *et al.*, 2006). CA1 pyramidal cells are more prominently tagged by memory-associated eYFP than CA3 or dentate gyrus cells (Fig. 3A), in line with PKM $\zeta$ -immunohistochemistry (Fig. 2C, D).

Then to examine the subcellular location within the memory-tagged CA1 pyramidal cells, we used the membrane-targeting ChR2-eYFP as the transgene in ArcCreER<sup>T2</sup>-ChR2-eYFP mice. Because of the dense labeling in the neuropil by the Chr2-eYFP, we used expansion microscopy to better visualize the dendritic processes of single CA1 pyramidal cells (Chen *et al.*, 2015). PKM $\zeta$  colocalizes at dendritic spines of memory-tagged cells that are labeled by ChR2-eYFP, providing direct evidence that PKM $\zeta$  is in dendritic spines in memory-tagged cells (Fig. 3B).

#### *Persistent increased PKM $\zeta$ in 1-month spatial memory storage*

Repeated active place avoidance conditioning at a 10-day-interval produces remote hippocampus-dependent spatial memory lasting 1 month (Pastalkova *et al.*, 2006; Hsieh *et al.*, 2017) (Fig. 4A). Mice were trained by a 30-min habituation trial, followed by three 30-min training trials with 2 h intertrial intervals, and another 3 training trials were given 10 days after day 1. Memory was tested 30 days after the last training trial. Significant effects are of training phase (pretraining, the end of training, and retention,  $F_{2,32} = 7.07, P = 0.0029$ ), treatment (control and trained,  $F_{1,16} = 26.29, P < 0.0001$ ), and their interaction ( $F_{2,32} = 7.29, P = 0.0025$ ). The retention performance is significantly different (post-hoc test,  $P = 0.0018$ ; untrained control,  $n = 11$ , trained,  $n = 7$ ).

In line with previous work using quantitative immunoblotting of rat hippocampus (Hsieh *et al.*, 2017), PKM $\zeta$ -immunoblotting of mouse hippocampus shows persistent increases 1 month after the last training session, as compared to untrained controls ( $t_{10} = 2.65, P = 0.024$ ,  $n$ 's = 6) (Fig. 4B).

PKM $\zeta$ -immunohistochemistry reveals that the trained group has higher CA1 PKM $\zeta$  intensity than untrained controls ( $n$ 's = 4,  $t_6 = 2.48, P = 0.048$ ) (Fig. C, D). Inspection outside the hippocampal formation reveals increased PKM $\zeta$  in deep layers of overlying somatosensory neocortex, as well as in retrosplenial cortex, but not in superficial layers as was observed a day after training.

## **Discussion**

In this study we visualized the amount and distribution of PKM $\zeta$  in the hippocampal formation during the maintenance of LTP and spatial long-term memory storage. In LTP, PKM $\zeta$  forms long-lasting traces in CA1 pyramidal cell bodies and dendrites for at least 2 h (Fig. 1). During spatial long-term memory, the traces of increased PKM $\zeta$  can last from 1 day (Fig. 2) to at least 1 month (Fig. 4), which is, to our knowledge, the longest duration of a change in a protein documented in spatial memory storage. Because increased PKM $\zeta$  is sufficient to potentiate synaptic transmission and intrahippocampal application of PKM $\zeta$  inhibitors reverse the maintenance of late-LTP and the memory of active place avoidance conditioning at 1 day and 1 month post-training (Ling *et al.*, 2002; Pastalkova *et al.*, 2006; Tsokas *et al.*, 2016), the loci of persistent increased PKM $\zeta$  likely represent sites of the endogenous molecular mechanism of LTP maintenance that sustain spatial long-term memory.

The mechanisms maintaining increased  $\text{PKM}\zeta$  in LTP might include the local synthesis of  $\text{PKM}\zeta$  from its dendritic mRNA, similar to the local increases in total CaMKII seen in dendrites 30 min after tetanization in LTP (Ouyang *et al.*, 1997), and the synaptic tagging and capture of the newly synthesized  $\text{PKM}\zeta$  to recently activated postsynaptic sites (Sajikumar *et al.*, 2005; Palida *et al.*, 2015). In LTP,  $\text{PKM}\zeta$  also appears persistently increased in cell bodies during LTP maintenance. These increases might represent sites of other long-term actions of  $\text{PKM}\zeta$  important for neuronal plasticity and memory maintenance, including epigenetic control of gene transcription in nuclei (Hernandez *et al.*, 2014; Ko *et al.*, 2016).

Spatial conditioning induces increases of  $\text{PKM}\zeta$  in CA1 that persist into remote memory. These observations indicate the Schaffer collateral/commissural CA3 pathways to CA1 is a candidate site for the long-term storage of information that is crucial for expressing the conditioned place avoidance, consistent with the prior observation of maintained synaptic potentiation of this pathway for at least 1 month, but only if the mouse expresses the remote place avoidance memory (Pavlowsky *et al.*, 2017). The localization of persistent increased  $\text{PKM}\zeta$  to the output neurons of the hippocampal formation in this spatial task is analogous to the persistent  $\text{PKM}\zeta$  increases observed in the output layer of motor cortex across similar time periods of a reaching task (Gao *et al.*, 2018). Neocortical  $\text{PKM}\zeta$  also appears to increase in active place avoidance memory at both superficial and deep layers at the earlier time point, but less so at the superficial layers in remote memory, and at deep layers of retrosplenial cortex during remote memory, but not at the earlier time. These potential system-level changes in  $\text{PKM}\zeta$  outside the hippocampus will require future study.

In contrast to CA1 with memory-related  $\text{PKM}\zeta$  increases, CA3 and dentate gyrus do not show changes in  $\text{PKM}\zeta$  during spatial long-term memory storage. This result and the related observation that CA3 cells are only weakly tagged by Arc activation during expression of memory is perhaps surprising given the prominent role of the recurrent collaterals of CA3 pyramidal cells in theories of hippocampal memory storage (McNaughton & Morris, 1987; Jensen & Lisman, 1996; Rolls, 1996; Papp *et al.*, 2007). It is possible that molecules in addition to  $\text{PKM}\zeta$ , such as CaMKII (Ouyang *et al.*, 1997; Lisman, 2017) or other PKCs (Hsieh *et al.*, 2017), may play roles in long-term memory storage in CA3. However, because spatial conditioning induces neither traces of  $\text{PKM}\zeta$  nor memory-tagged cells in CA3, this region might play a role in storing short-term rather than long-term memories for active place avoidance (Gilbert & Kesner, 2006). Alternatively, the proportion of neurons with increased  $\text{PKM}\zeta$  might be too small to detect by our techniques outside CA1. This may be the case particularly in dentate gyrus, where there is a suggestion of increased  $\text{PKM}\zeta$  in its suprapyramidal blade early in memory storage (Fig. 2D), which does not reach statistical significance.

Lastly, although some authors have argued that a half-life of  $\text{PKM}\zeta$  shorter than a very long-term memory lasting weeks makes it an unlikely molecular memory storage mechanism (Palida *et al.*, 2015), our results show that this is not necessarily the case. Information at the molecular level can be stored as a persistent increase or decrease in the steady-state level or conformation of a protein. Thus, even though the half-life of  $\text{PKM}\zeta$  may be days *in vivo*, as suggested by shRNA (Dong *et al.*, 2015; Wang *et al.*, 2016) and inducible genetic knockdowns (Volk *et al.*, 2013), the steady-state increases of  $\text{PKM}\zeta$  protein can last a month (Fig. 4) (Hsieh *et al.*, 2017; Gao *et al.*, 2018). Indeed, even in primary cultures of neurons, in which the  $\text{PKM}\zeta$  half-life has been determined, the steady-state increases of  $\text{PKM}\zeta$  induced by chemical-LTP

outlast the half-life of individual  $\text{PKM}\zeta$  protein molecules (Palida *et al.*, 2015). The sustained steady-state increases in  $\text{PKM}\zeta$  that we and others observe can be due to positive feedback loops that persistently increase its synthesis (Westmark *et al.*, 2010; Jalil *et al.*, 2015; Helfer & Shultz, 2018) or decrease its turnover (Vogt-Eisele *et al.*, 2013), or both. Remarkably, our results with memory-labeled neurons suggest the possibility that these steady-state increases may be compartmentalized within spines (Fig. 3B). Further work will be necessary to examine the kinetics of  $\text{PKM}\zeta$  turnover within the dendritic compartments of memory-storing neurons.

### **Conflict of interests**

The authors declare no competing financial interests with respect to authorship or the publication of this article.

### **Supporting Information**

Additional supporting information can be found in the online version of this article.

### **Data Accessibility**

Research data will be made available on request to the corresponding authors.

### **Acknowledgements**

We gratefully acknowledge support from grants provided by NIH grants R37 MH057068 (T.C.S.), R01 MH115304 (T.C.S., A.A.F.), and R01 NS108190 (P.B., T.C.S.).

### **Author contributions**

C.H. and P.T. contributed equally to this study, T.C.S, A.A.F., A.C., C.G.-J., E.L., N.S.B., C.A.D., P.B., J.E.C., C.H., and P.T. conceived the study and designed the methodology. C.H., P.T., A.C., C.G.-J., E.L., N.S.B., C.A.D., performed the experiments. C.H., P.T., A.C., C.G.-J., E.L., N.S.B., C.A.D., R.E.F.-O., L.M.R.V., A.A.F. and T.C.S. performed the analyses of the experimental data. T.C.S. and A.A.F. wrote the article with contributions and input from P.T., C.H., and C.A.D.

### **Abbreviations**

DG, dentate gyrus; eYFP, enhanced yellow fluorescent protein; fEPSPs, field excitatory postsynaptic potentials; LTP, long-term potentiation; PKC, protein kinase C;  $\text{PKM}\zeta$ , protein kinase Mzeta; SEM, standard error of mean.

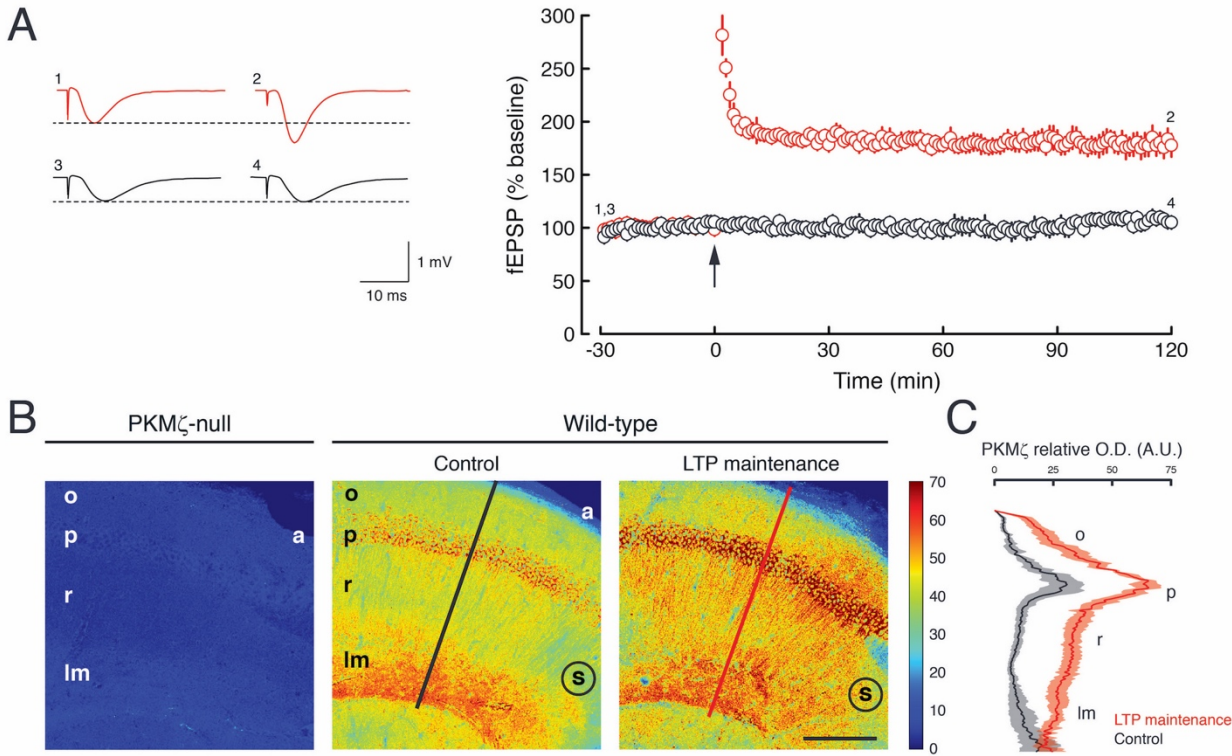
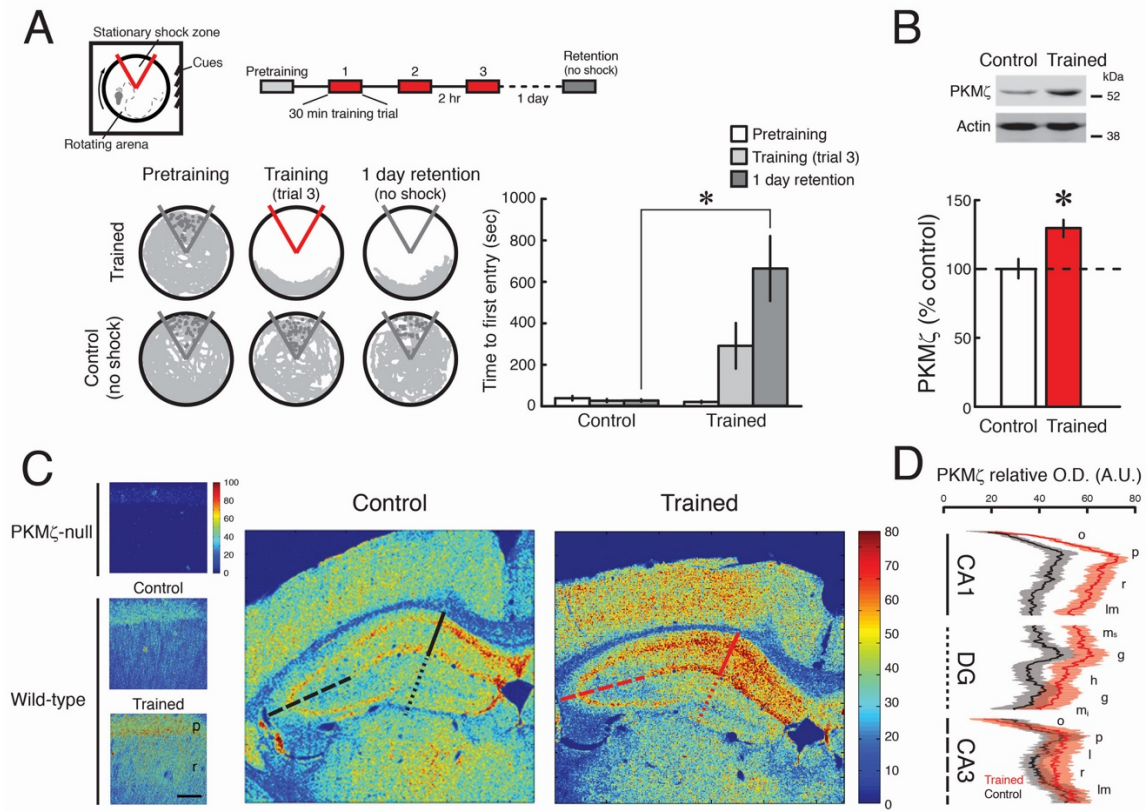


FIG. 1. Persistent increased PKM $\zeta$  in LTP maintenance. (A) Time-course of LTP (shown in red) and untetanized controls (shown in black). Left, representative fEPSPs correspond to numbered time points in time-course at right. Tetanization of Schaffer collateral/commissural afferent fibers is at arrow. Control slices are from the same hippocampus as tetanized slices and receive test stimulation for equivalent periods of time. (B) Representative immunohistochemistry of hippocampal CA1 subfield. Left, minimal background immunostaining in CA1 from PKM $\zeta$ -null mouse. Middle, PKM $\zeta$  in untetanized control slice from wild-type mouse, as recorded in (A). Black line corresponds to location of profile shown in (C). Right, persistent increased PKM $\zeta$  2 h post-tetanization in slice from wild-type mouse. Red line corresponds to location of profile shown in (C). Colormap is shown as inset at right. Scale bar = 200  $\mu$ m; s, placement of stimulating electrode at CA3/CA1 border; a, alveus; o, stratum oriens; p, stratum pyramidale; r, stratum radiatum; Im, stratum lacunosum-moleculare. (C) Profiles shows increase in PKM $\zeta$  in LTP maintenance (red), compared to untetanized controls (black). Mean  $\pm$  SEM; n and statistics reported in Results. O.D., optical density; A.U., arbitrary units.



**FIG. 2. Persistent increased PKM $\zeta$  in spatial long-term memory storage.** (A) Above, left, schematic of active place avoidance apparatus. Above, right, schematic of spatial conditioning protocol. Active place avoidance conditioning produces spatial long-term memory at 1 day post-training, measured as increase in time to first entry into the shock zone. Below left, representative paths of initial 10 min during pretraining, the trial at the end of training, and during retention testing with the shock off 1 day after training. The shock zone is shown in red with shock on, and gray with shock off. Gray circles denote where shocks would have been received if the shock were on. Right, time to first entry measure of active place avoidance memory (mean  $\pm$  SEM; \*, statistical significance, as reported in Results). (B) PKM $\zeta$  increases 1 day post-training in dorsal hippocampus as measured by immunoblot. Above, representative immunoblots show increases in PKM $\zeta$  between control untrained mouse and trained mouse, and actin as loading control. Below, mean data; the level of protein in the untrained control hippocampi is set to 100%. Mean  $\pm$  SEM; \*denotes significance. (C) Representative data show PKM $\zeta$  increases 1 day post-training in dorsal hippocampus as measured by immunohistochemistry. Left, Above, PKM $\zeta$  immunohistochemistry of PKM $\zeta$ -null hippocampus shows minimal background immunostaining. Left, middle and below, PKM $\zeta$  immunohistochemistry of wild-type hippocampi from untrained and trained mice show increased PKM $\zeta$ -immunostaining in stratum pyramidale (p) and stratum radiatum (r) of trained mouse. Colormap is shown as insert at right. Right, spatial training increases PKM $\zeta$  immunostaining in CA1, but not CA3 or dentate gyrus. Hippocampal formation from control untrained wild-type mouse shows widespread staining in hippocampal formation. Black lines correspond to location of profiles of untrained controls shown in (D). Red lines correspond to location of profiles of

trained animals shown in (D). The  $\text{PKM}\zeta$  intensity is examined across CA1 (solid line), DG (dotted line), and CA3 (dashed line). Colormap is shown as insert at right. Scale bar: left panels =  $60 \mu\text{m}$ ; right panels =  $300 \mu\text{m}$ . (D) Profiles shows increase in  $\text{PKM}\zeta$  in CA1, and not in dentate gyrus (DG) or CA3 after training (red), compared to untrained controls (black). Mean data  $\pm$  SEM; statistical significance reported in Results.

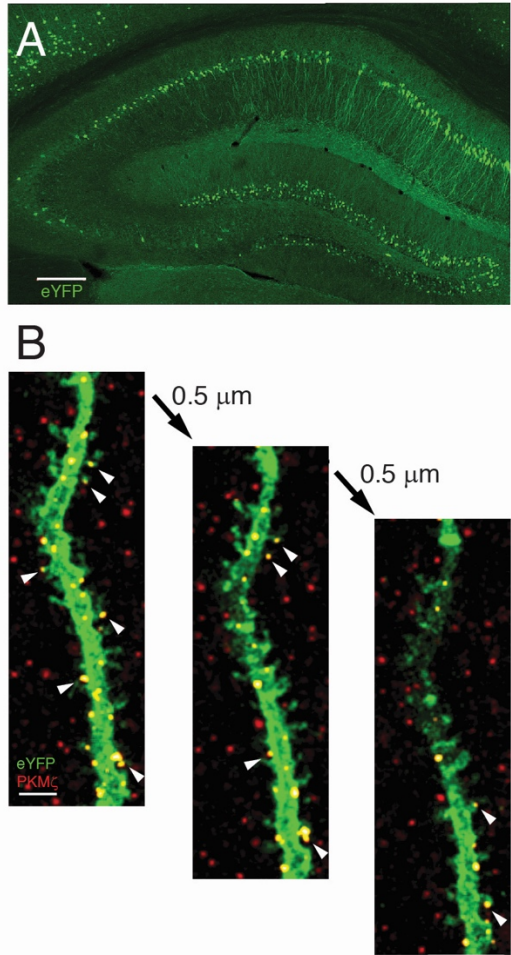


FIG. 3. Persistent increased  $\text{PKM}\zeta$  in memory-associated cells during spatial long-term memory storage. (A) Dorsal hippocampus expression of eYFP in an ArcCre-eYFP mouse after active place avoidance training. To establish a long-term memory, the mouse was exposed to a 30-min pretraining session followed by three 30-min training trials the next day. To label cells, tamoxifen was injected on day 3, 5 h prior to a fourth 30-min training trial. On day 8, retention was tested, and the mouse was sacrificed 1 h afterwards. The times to first enter the location of shock for this mouse were: pretrain: 14s; trials days 2-3 and 8: 21, 38, 32, 229, 167s, respectively. By inspection, it is evident that a minority subset of neurons is labeled in hippocampus, as expected, but that CA1 appears to express more memory-associated eYFP than DG, which is more than CA3. Scale bar = 200  $\mu\text{m}$ . (B) Half-micron z-stack series of three confocal images of a CA1 dendrite in a hippocampus slice from an ArcCre-ChR2-eYFP mouse. The tissue was prepared for imaging by expansion microscopy. The image illustrates  $\text{PKM}\zeta$  puncta in dendritic spines (yellow, at arrowheads) of a neuron that expresses eYFP in response to Arc-mediated Cre activation of ChR2-eYFP expression. Scale bar = 10  $\mu\text{m}$ .

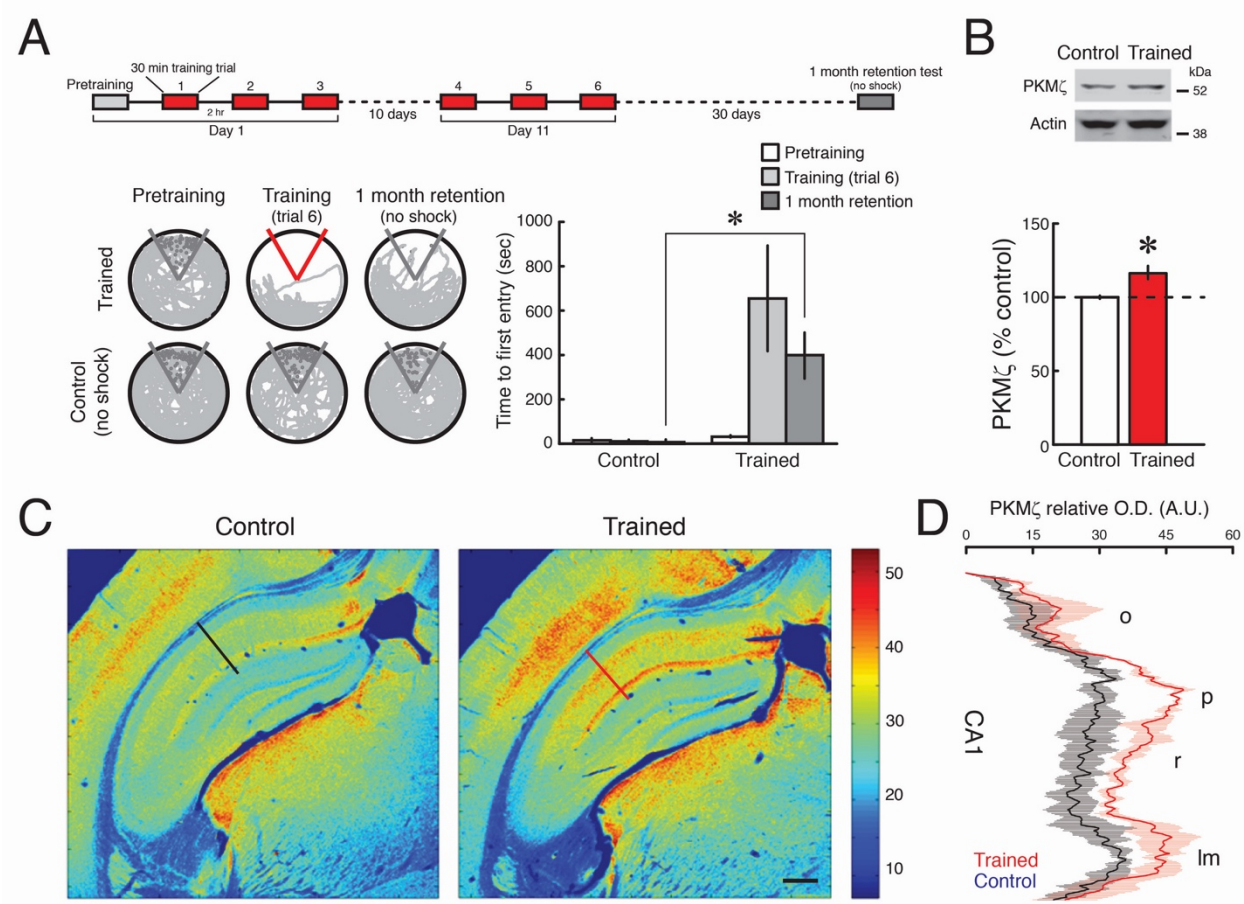


FIG. 4. Persistent increased PKM $\zeta$  in 1-month spatial remote memory storage. (A) Above, schematic of spatial conditioning protocol; repeated conditioning separated by 1 week produces remote memory lasting 30 days. Below left, representative paths during pretraining, the trial at the end of training, and during retention testing with the shock off 30 days after training. The shock zone is shown in red with shock on, and gray with shock off. Gray circles denote where shocks would have been received if the shock were on. Right, time to first entry measure of active place avoidance memory (mean  $\pm$  SEM; \*, statistical significance, as reported in Results). (B) PKM $\zeta$  increases 30 days post-training in dorsal hippocampus as measured by immunoblot. Above, representative immunoblots show increases in PKM $\zeta$  between control untrained mouse and trained mouse, and actin as loading control. Below, mean data show the levels of protein in the untrained control hippocampi set at 100%. Mean  $\pm$  SEM; \*denotes significance. (C) Representative data show PKM $\zeta$  increases 30 days post-training in CA1 as measured by immunohistochemistry. Black line in control mouse and red line in trained mouse correspond to locations of profiles shown in (D). Colormap is shown as insert at right. Scale bar = 300  $\mu$ m. (D) Profiles shows increase in PKM $\zeta$  30 days after training (red), compared to untrained controls (black). Mean data  $\pm$  SEM; statistical significance reported in Results.

## References

Anderson, W.W. & Collingridge, G.L. (2007) Capabilities of the WinLTP data acquisition program extending beyond basic LTP experimental functions. *J Neurosci Methods*, **162**, 346-356.

Chen, F., Tillberg, P.W. & Boyden, E.S. (2015) Optical imaging. Expansion microscopy. *Science*, **347**, 543-548.

Chung, A., Garcia-Jou, C., Dvorak, D., Hussain, N. & Fenton, A.A. (2019) Learning to learn persistently modifies a neocortical-hippocampal excitatory-inhibitory subcircuit. *BioRxiv*, 817627.

Denny, C.A., Kheirbek, M.A., Alba, E.L., Tanaka, K.F., Brachman, R.A., Laughman, K.B., Tomm, N.K., Turi, G.F., Losonczy, A. & Hen, R. (2014) Hippocampal memory traces are differentially modulated by experience, time, and adult neurogenesis. *Neuron*, **83**, 189-201.

Dong, Z., Han, H., Li, H., Bai, Y., Wang, W., Tu, M., Peng, Y., Zhou, L., He, W., Wu, X., Tan, T., Liu, M., Wu, X., Zhou, W., Jin, W., Zhang, S., Sacktor, T.C., Li, T., Song, W. & Wang, Y.T. (2015) Long-term potentiation decay and memory loss are mediated by AMPAR endocytosis. *The Journal of clinical investigation*, **125**, 234-247.

Gao, P.P., Goodman, J.H., Sacktor, T.C. & Francis, J.T. (2018) Persistent increases of PKM $\zeta$  in sensorimotor cortex maintain procedural long-term memory storage. *iScience*, **5**, 90-98.

Gilbert, P.E. & Kesner, R.P. (2006) The role of the dorsal CA3 hippocampal subregion in spatial working memory and pattern separation. *Behavioural brain research*, **169**, 142-149.

Guzowski, J.F., McNaughton, B.L., Barnes, C.A. & Worley, P.F. (1999) Environment-specific expression of the immediate-early gene Arc in hippocampal neuronal ensembles. *Nat Neurosci*, **2**, 1120-1124.

Guzowski, J.F., Miyashita, T., Chawla, M.K., Sanderson, J., Maes, L.I., Houston, F.P., Lipa, P., McNaughton, B.L., Worley, P.F. & Barnes, C.A. (2006) Recent behavioral history modifies coupling between cell activity and Arc gene transcription in hippocampal CA1 neurons. *Proc Natl Acad Sci U S A*, **103**, 1077-1082.

Helper, P. & Shultz, T.R. (2018) Coupled feedback loops maintain synaptic long-term potentiation: A computational model of PKMzeta synthesis and AMPA receptor trafficking. *PLoS Comput Biol*, **14**, e1006147.

Hernandez, A.I., Blace, N., Crary, J.F., Serrano, P.A., Leitges, M., Libien, J.M., Weinstein, G., Tcherapanov, A. & Sacktor, T.C. (2003) Protein kinase M $\zeta$  synthesis from a brain mRNA encoding an independent protein kinase C $\zeta$  catalytic domain. Implications for the molecular mechanism of memory. *J Biol Chem*, **278**, 40305-40316.

Hernandez, A.I., Oxberry, W.C., Crary, J.F., Mirra, S.S. & Sacktor, T.C. (2014) Cellular and subcellular localization of PKMzeta. *Philosophical transactions of the Royal Society of London. Series B, Biological sciences*, **369**, 20130140.

Hsieh, C., Tsokas, P., Serrano, P., Hernandez, A.I., Tian, D., Cottrell, J.E., Shouval, H.Z., Fenton, A.A. & Sacktor, T.C. (2017) Persistent increased PKMzeta in long-term and remote spatial memory. *Neurobiology of learning and memory*, **138**, 135-144.

Jalil, S.J., Sacktor, T.C. & Shouval, H.Z. (2015) Atypical PKCs in memory maintenance: the roles of feedback and redundancy. *Learning & memory*, **22**, 344-353.

Jensen, O. & Lisman, J.E. (1996) Hippocampal CA3 region predicts memory sequences: accounting for the phase precession of place cells. *Learning & memory*, **3**, 279-287.

Ko, H.G., Kim, J.I., Sim, S.E., Kim, T., Yoo, J., Choi, S.L., Baek, S.H., Yu, W.J., Yoon, J.B., Sacktor, T.C. & Kaang, B.K. (2016) The role of nuclear PKMzeta in memory maintenance. *Neurobiology of learning and memory*, **135**, 50-56.

Lacagnina, A.F., Brockway, E.T., Crovetti, C.R., Shue, F., McCarty, M.J., Sattler, K.P., Lim, S.C., Santos, S.L., Denny, C.A. & Drew, M.R. (2019) Distinct hippocampal engrams control extinction and relapse of fear memory. *Nat Neurosci*, **22**, 753-761.

Lesburgueres, E., Sparks, F.T., O'Reilly, K.C. & Fenton, A.A. (2016) Active place avoidance is no more stressful than unreinforced exploration of a familiar environment. *Hippocampus*, **26**, 1481-1485.

Ling, D.S., Benardo, L.S., Serrano, P.A., Blace, N., Kelly, M.T., Crary, J.F. & Sacktor, T.C. (2002) Protein kinase M $\zeta$  is necessary and sufficient for LTP maintenance. *Nat Neurosci*, **5**, 295-296.

Lisman, J. (2017) Criteria for identifying the molecular basis of the engram (CaMKII, PKMzeta). *Molecular brain*, **10**, 55.

McNaughton, B.L. & Morris, R.G.M. (1987) Hippocampal synaptic enhancement and information storage within a distributed memory system. *Trends Neurosci*, **10**, 409-415.

Muslimov, I.A., Nimmrich, V., Hernandez, A.I., Tcherepanov, A., Sacktor, T.C. & Tiedge, H. (2004) Dendritic transport and localization of protein kinase M $\zeta$  mRNA: Implications for molecular memory consolidation. *J Biol Chem*, **279**, 52613-52622.

Osten, P., Valsamis, L., Harris, A. & Sacktor, T.C. (1996) Protein synthesis-dependent formation of protein kinase M $\zeta$  in long-term potentiation. *J Neurosci*, **16**, 2444-2451.

Ouyang, Y., Kantor, D., Harris, K.M., Schuman, E.M. & Kennedy, M.B. (1997) Visualization of the distribution of autophosphorylated calcium/calmodulin-dependent protein kinase II after tetanic stimulation in the CA1 area of the hippocampus. *J Neurosci*, **17**, 5416-5427.

Palida, S.F., Butko, M.T., Ngo, J.T., Mackey, M.R., Gross, L.A., Ellisman, M.H. & Tsien, R.Y. (2015) PKMzeta, But Not PKClambda, Is Rapidly Synthesized and Degraded at the Neuronal Synapse. *J Neurosci*, **35**, 7736-7749.

Papp, G., Witter, M.P. & Treves, A. (2007) The CA3 network as a memory store for spatial representations. *Learning & memory*, **14**, 732-744.

Pastalkova, E., Serrano, P., Pinkhasova, D., Wallace, E., Fenton, A.A. & Sacktor, T.C. (2006) Storage of spatial information by the maintenance mechanism of LTP. *Science*, **313**, 1141-1144.

Pavlowsky, A., Wallace, E., Fenton, A.A. & Alarcon, J.M. (2017) Persistent modifications of hippocampal synaptic function during remote spatial memory. *Neurobiology of learning and memory*, **138**, 182-197.

Perusini, J.N., Cajigas, S.A., Cohensedgh, O., Lim, S.C., Pavlova, I.P., Donaldson, Z.R. & Denny, C.A. (2017) Optogenetic stimulation of dentate gyrus engrams restores memory in Alzheimer's disease mice. *Hippocampus*, **27**, 1110-1122.

Rolls, E.T. (1996) A theory of hippocampal function in memory. *Hippocampus*, **6**, 601-620.

Sacktor, T.C. & Fenton, A.A. (2018) What does LTP tell us about the roles of CaMKII and PKMzeta in memory? *Molecular brain*, **11**, 77.

Sacktor, T.C., Osten, P., Valsamis, H., Jiang, X., Naik, M.U. & Sublette, E. (1993) Persistent activation of the  $\zeta$  isoform of protein kinase C in the maintenance of long-term potentiation. *Proc Natl Acad Sci USA*, **90**, 8342-8346.

Sajikumar, S., Navakkode, S., Sacktor, T.C. & Frey, J.U. (2005) Synaptic tagging and cross-tagging: the role of protein kinase M $\zeta$  in maintaining long-term potentiation but not long-term depression. *J Neurosci*, **25**, 5750-5756.

Srinivas, S., Watanabe, T., Lin, C.S., William, C.M., Tanabe, Y., Jessell, T.M. & Costantini, F. (2001) Cre reporter strains produced by targeted insertion of EYFP and ECFP into the ROSA26 locus. *BMC Dev Biol*, **1**, 4.

Tsokas, P., Grace, E.A., Chan, P., Ma, T., Sealfon, S.C., Iyengar, R., Landau, E.M. & Blitzer, R.D. (2005) Local protein synthesis mediates a rapid increase in dendritic elongation factor 1A after induction of late long-term potentiation. *J Neurosci*, **25**, 5833-5843.

Tsokas, P., Hsieh, C., Yao, Y., Lesburgueres, E., Wallace, E.J., Tcherepanov, A., Jothianandan, D., Hartley, B.R., Pan, L., Rivard, B., Farese, R.V., Sajan, M.P., Bergold, P.J., Hernandez, A.I., Cottrell, J.E., Shouval, H.Z., Fenton, A.A. & Sacktor, T.C. (2016) Compensation for PKMzeta in long-term potentiation and spatial long-term memory in mutant mice. *eLife*, **5**.

Tsokas, P., Ma, T., Iyengar, R., Landau, E.M. & Blitzer, R.D. (2007) Mitogen-activated protein kinase upregulates the dendritic translation machinery in long-term potentiation by controlling the mammalian target of rapamycin pathway. *J Neurosci*, **27**, 5885-5894.

Tsokas, P., Rivard, B., Hsieh, C., Cottrell, J.E., Fenton, A.A. & Sacktor, T.C. (2019) Antisense Oligodeoxynucleotide Perfusion Blocks Gene Expression of Synaptic Plasticity-related Proteins without Inducing Compensation in Hippocampal Slices. *Bio Protoc*, **9**.

Vogt-Eisele, A., Kruger, C., Duning, K., Weber, D., Spoelgen, R., Pitzer, C., Plaas, C., Eisenhardt, G., Meyer, A., Vogt, G., Krieger, M., Handwerker, E., Wennmann, D.O., Weide, T., Skryabin, B.V., Klugmann, M., Pavenstadt, H., Huentelmann, M.J., Kremerskothen, J. & Schneider, A. (2013) KIBRA (KIdney/BRAin protein) regulates learning and memory and stabilizes Protein kinase Mzeta. *Journal of neurochemistry*.

Volk, L.J., Bachman, J.L., Johnson, R., Yu, Y. & Huganir, R.L. (2013) PKM-zeta is not required for hippocampal synaptic plasticity, learning and memory. *Nature*, **493**, 420-423.

Wang, S., Sheng, T., Ren, S., Tian, T. & Lu, W. (2016) Distinct Roles of PKC $\iota$ /lambda and PKMzeta in the Initiation and Maintenance of Hippocampal Long-Term Potentiation and Memory. *Cell Rep*, **16**, 1954-1961.

Westmark, P.R., Westmark, C.J., Wang, S., Levenson, J., O'Riordan, K.J., Burger, C. & Malter, J.S. (2010) Pin1 and PKMzeta sequentially control dendritic protein synthesis. *Sci Signal*, **3**, ra18.